



HAL
open science

TAFA4, a Chemokine-like Protein, Modulates Injury-Induced Mechanical and Chemical Pain Hypersensitivity in Mice

Marie-Claire Delfini, Annabelle Mantilleri, Stéphane Gaillard, Jizhe Hao, Ana Reynders, Pascale Malapert, Serge Alonso, Amaury François, Christian Barrère, Rebecca Seal, et al.

► **To cite this version:**

Marie-Claire Delfini, Annabelle Mantilleri, Stéphane Gaillard, Jizhe Hao, Ana Reynders, et al.. TAFA4, a Chemokine-like Protein, Modulates Injury-Induced Mechanical and Chemical Pain Hypersensitivity in Mice. *Cell Reports*, 2013, 5 (2), pp.378-388. 10.1016/j.celrep.2013.09.013 . hal-02370525

HAL Id: hal-02370525

<https://hal.science/hal-02370525v1>

Submitted on 19 Nov 2019

HAL is a multi-disciplinary open access archive for the deposit and dissemination of scientific research documents, whether they are published or not. The documents may come from teaching and research institutions in France or abroad, or from public or private research centers.

L'archive ouverte pluridisciplinaire **HAL**, est destinée au dépôt et à la diffusion de documents scientifiques de niveau recherche, publiés ou non, émanant des établissements d'enseignement et de recherche français ou étrangers, des laboratoires publics ou privés.

TAFA4, a Chemokine-like Protein, Modulates Injury-Induced Mechanical and Chemical Pain Hypersensitivity in Mice

Marie-Claire Delfini,^{1,8} Annabelle Mantilleri,^{1,8} Stéphane Gaillard,¹ Jizhe Hao,² Ana Reynders,¹ Pascale Malapert,¹ Serge Alonso,¹ Amaury François,³ Christian Barrere,³ Rebecca Seal,⁴ Marc Landry,^{5,6} Alain Eschallier,⁷ Abdelkrim Alloui,⁷ Emmanuel Bourinet,³ Patrick Delmas,² Yves Le Feuvre,^{5,6} and Aziz Moqrich^{1,*}

¹Aix-Marseille-Université, CNRS, Institut de Biologie du Développement de Marseille, UMR 7288, case 907, 13288 Marseille Cedex 09, France

²Aix-Marseille-Université, CNRS, Centre de Recherche en Neurobiologie et Neurophysiologie de Marseille, UMR 7286, CS80011, Bd Pierre Dramard, 13344 Marseille Cedex 15, France

³Laboratories of Excellence, Ion Channel Science and Therapeutics, Institut de Génomique Fonctionnelle, UMR 5203, CNRS, U661, INSERM, Universités Montpellier I and II, 141 Rue de la Cardonille, 34094 Montpellier Cedex 05, France

⁴Departments of Neurobiology and Otolaryngology, Center for Pain Research, University of Pittsburgh, Pittsburgh, PA 15213-2536, USA

⁵University Bordeaux, Interdisciplinary Institute for Neuroscience, UMR 5297, 33000 Bordeaux, France

⁶CNRS, Interdisciplinary Institute for Neuroscience, UMR 5297, 33000 Bordeaux, France

⁷Laboratoire de Pharmacologie Médicale, Faculté de Médecine et de Pharmacie, UMR 766 INSERM, 28 place Henri-Dunant, BP 38, 63001 Clermont-Ferrand Cedex 1, France

⁸These authors contributed equally to this work

*Correspondence: aziz.moqrich@univ-amu.fr
<http://dx.doi.org/10.1016/j.celrep.2013.09.013>

This is an open-access article distributed under the terms of the Creative Commons Attribution-NonCommercial-No Derivative Works License, which permits non-commercial use, distribution, and reproduction in any medium, provided the original author and source are credited.

SUMMARY

C-low-threshold mechanoreceptors (C-LTMRs) are unique among C-unmyelinated primary sensory neurons. These neurons convey two opposite aspects of touch sensation: a sensation of pleasantness, and a sensation of injury-induced mechanical pain. Here, we show that TAFA4 is a specific marker of C-LTMRs. Genetic labeling in combination with electrophysiological recordings show that TAFA4⁺ neurons have intrinsic properties of mechano-nociceptors. TAFA4-null mice exhibit enhanced mechanical and chemical hypersensitivity following inflammation and nerve injury as well as increased excitability of spinal cord lamina II neurons, which could be reversed by intrathecal or bath application of recombinant TAFA4 protein. In wild-type C57/Bl6 mice, intrathecal administration of TAFA4 strongly reversed carrageenan-induced mechanical hypersensitivity, suggesting a potent analgesic role of TAFA4 in pain relief. Our data provide insights into how C-LTMR-derived TAFA4 modulates neuronal excitability and controls the threshold of somatic sensation.

INTRODUCTION

Touch is essential for a myriad of behaviors that range from avoiding harmful stimuli to social bonds. Touch sensation is

mediated by a variety of morphologically and physiologically specialized subpopulations of cutaneous afferents known as low-threshold mechanoreceptors (LTMRs). These afferent fibers have their cell bodies clustered in the dorsal root ganglia (DRG) in the trunk and in the trigeminal ganglia (TG) in the head. Their pseudounipolar organization allows protrusion of two distinct axonal branches: one extending to specialized end organs in the periphery, and the other penetrating the spinal cord to synapse with second-order neurons (Li et al., 2011; Lumpkin et al., 2010). Based on their axon caliber, degree of myelination, speed of action potential (AP) propagation, mechanical threshold, and the rate of adaptation to sustained mechanical stimuli, LTMRs can be split into A β , A δ , or C fibers (Bessou and Perl, 1969; Li et al., 2011; Smith and Lewin, 2009; Zimmermann et al., 2009). Although A β -LTMR afferents are widely accepted to mediate discriminative touch, the functional role of C-LTMR afferents is just emerging. C-LTMR afferents were first identified in the hairy skin of the cat and the monkey (Zotterman, 1939) and later in humans and mice (Bessou et al., 1971; Douglas and Ritchie, 1957; Johansson et al., 1988; Li et al., 2011; Maruhashi et al., 1952; Seal et al., 2009; Zotterman, 1939). Recent studies have shown that these neurons specifically express tyrosine hydroxylase (TH) and the vesicular glutamate transporter 3 (VGLUT3) and have afferent branches that project to the innermost layer of lamina II of the dorsal horn of the spinal cord and provide rich innervation of trunk and limb hairy skin (Li et al., 2011; Seal et al., 2009). C-LTMRs have been proposed to contribute to touch hypersensitivity after injury in mice (Liljencrantz et al., 2013; Seal et al., 2009) and to an affective or emotional component of touch in humans (Löken et al., 2009;

Olausson et al., 2002). These data suggest that C-LTMRs have dual functions: a function of pleasantness under normal conditions that can be converted to pain under pathological conditions. Despite recent advances (Nagi et al., 2011; Seal et al., 2009), the mechanisms controlling this functional duality are poorly understood.

In a recent study, we have identified several genes defining discrete subsets of small diameter nonpeptidergic nociceptors (Legha et al., 2010). Here, we demonstrate that TFAFA4, a chemokine-like secreted protein (Tom Tang et al., 2004), is specifically expressed in C-LTMRs. Whole-cell recording of fluorescently labeled TFAFA4-expressing neurons confirmed that this subset of neurons displays many properties of C-unmyelinated mechano-nociceptors. TFAFA4-null mice are viable and respond normally to a variety of acute thermal and mechanical somatic sensations but developed sustained mechanical and chemical hypersensitivity following tissue injury, both of which could be reversed by intrathecally (IT) applied human recombinant TFAFA4 protein. In wild-type (WT) C57/Bl6 mice, IT administration of TFAFA4 also reversed tissue injury mechanical hypersensitivity. In agreement with increased injury-induced hypersensitivity in TFAFA4-null mice, we found significant hyperexcitability of inner lamina II neurons in TFAFA4-null mice. Thus, under pathological conditions, C-LTMR-derived TFAFA4 modulates the threshold of activation of second-order spinal cord neurons, providing insights into the role of C-LTMRs in response to painful stimuli.

RESULTS

TFAFA4 Is a Specific Marker of C-LTMRs

In a previous study, we identified several genes expressed in discrete subsets of DRG neurons (Legha et al., 2010; Moqrich et al., 2004). Among them, *Tafa4* drew specific attention because (1) its transcripts were highly enriched in adult DRG and trigeminal neurons, (2) it marks a small subpopulation of neurons, and (3) it encodes a 100 amino acid-secreted proteins of unknown function that belong to a family of proteins composed of five highly homologous members named the “Tafa family” (Tom Tang et al., 2004).

Using in situ hybridization, we found *Tafa4* expressed in approximately 8% and 19% of total lumbar (L4) and thoracic (T12) adult DRG neurons, respectively (Figure 1A). Double-fluorescent labeling experiments showed that *Tafa4* is completely excluded from TrkA⁺ neurons and identified a subset of Ret⁺ neurons (Figures 1C and 1D). TFAFA4⁺ neurons do not bind IB4 and are completely distinct from *mrgprd*⁺ neurons (Figures 1E and 1F). In contrast, TFAFA4 is predominantly coexpressed with *TH* and *VGLUT3* (Figures 1G and 1H) and totally excluded from the newly described massage-like-activated MRGPRB4⁺ neurons (Vrontou et al., 2013) (data not shown). Using VGLUT3-EGFP DRG sections, we found that 92% ± 4% of TFAFA4⁺ neurons coexpress EGFP, and 94% ± 6% of EGFP⁺ neurons coexpress TFAFA4 (Figure 1H), identifying TFAFA4 as a specific marker of C-LTMRs. In contrast to TH and VGLUT3, TFAFA4 is almost restricted to DRG and trigeminal neurons with a low expression in CNS neurons, namely in the habenula and in scattered populations of neurons in the nuclei of the brain stem and hypothalamus (data not shown).

TFAFA4-Expressing Neurons Display Properties of Mechano-Nociceptors

To investigate the role of TFAFA4 in C-LTMRs, we have generated a knockin (KI) mouse model that allows us to genetically label TFAFA4-expressing neurons while eliminating TFAFA4 protein (Figure S1A). GFP⁺ neurons of heterozygous mice projected to the innermost layer of lamina II centrally and exclusively innervated the hairy part of the skin peripherally (Figures S1G–S1J).

Using patch-clamp recordings and calcium imaging, we found that GFP⁺ neurons displayed many properties of C-unmyelinated nociceptors, including small cell capacitance, high input resistance, short-duration AP devoid of prominent hump in the repolarizing phase, and a remarkable concomitant expression of TTX-resistant Nav1.8, low-threshold T-type Ca²⁺ (ICa_T), A-type K⁺ current (IK_A), and hyperpolarization-activated h (I_h) currents (Figures S2A–S2C). ICa_T-mediated rebound potentials were also typically observed at repolarization (Figure S2D). The activation of IK_A resulted in a delay in the occurrence of APs or rebound potentials in response to positive or negative current steps, respectively (Figure S2D). The homogeneous presence of these different currents shapes the cell firing in a unique way, with a depolarizing “sag” response to negative current steps due to I_h and a “gap” in AP firing in response to depolarizing current steps. These firing properties can be used as specific criteria to classify TFAFA4-expressing neurons.

GFP⁺ neurons did not respond to many putative nociceptive agents, including capsaicin, menthol, prenenolone sulfate, and 5HT or to rapid cooling (Figure S2E). In contrast, GFP⁺ neurons displayed differential responses to the TRPA1 agonist allyl isothiocyanate (AITC) and to hypoosmotic solution (Figure S2E; data not shown), suggesting some functional heterogeneity within C-LTMRs.

Classical features of C-LTMRs, including slow conduction velocities, trains of spikes in response to a light mechanical force, and slow adaptation to a sustained mechanical stimulus, have been determined using ex vivo skin nerve preparations (Bessou et al., 1971; Li et al., 2011; Seal et al., 2009; Woodbury et al., 2001). Application of mechanical forces to the cell body of GFP⁺ neurons revealed the presence of mechanically activated (MA) cation currents in 95% of neurons tested (Figures 2A and 2B). Although rapidly adapting MA currents could be occasionally encountered (15%), slow and ultraslowly adapting MA currents were predominant (21.3% and 57.9%, respectively) in GFP⁺ neurons (Figure 2A). All these currents were cationic and nonselective, with reversal potential ranging from –2 to +4 mV (data not shown). Consistent with the slow adaptation properties of MA currents, slow velocity ramp stimulus was able to trigger APs (Figure 2B), indicating that mechanosensory GFP⁺ neurons respond to slow motion stimuli. Taken together, our expression data, combined with calcium imaging and electrophysiological recordings, demonstrate that TFAFA4⁺ neurons display physiological properties of C-unmyelinated mechano-nociceptors.

TFAFA4 Is Dispensable for Molecular, Anatomical, and Physiological Properties of C-LTMRs

We first confirmed that TFAFA4 transcripts were completely abolished in TFAFA4^{GFP/GFP} homozygous mice (hereafter TFAFA4-null mice) (Figures S1B and S1C). Using SCG10 as a pan-neuronal

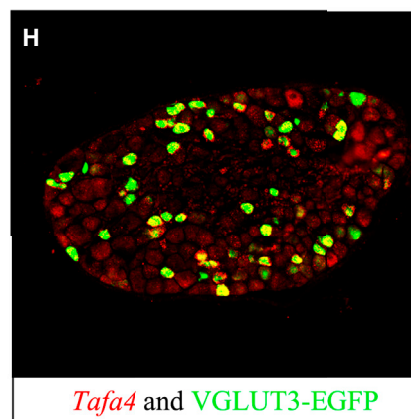
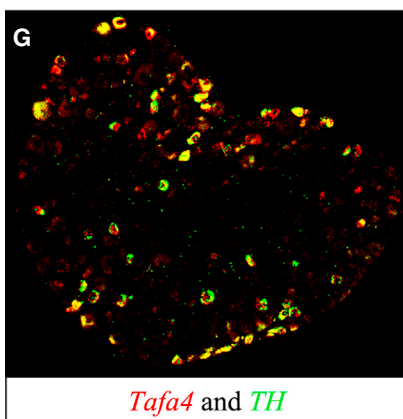
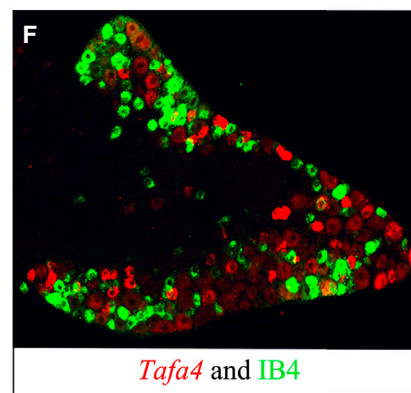
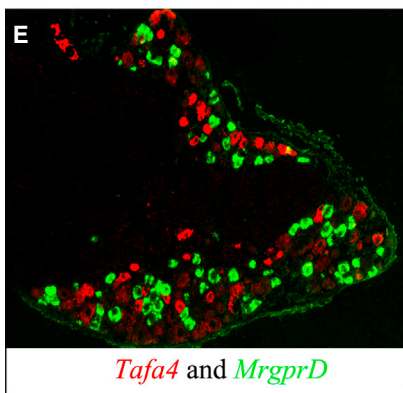
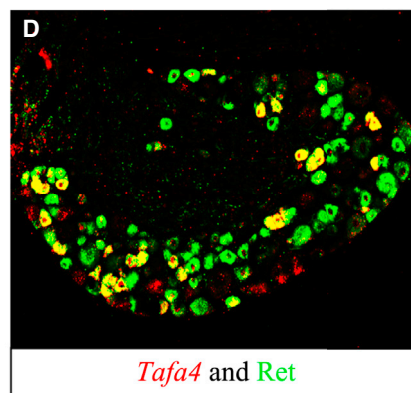
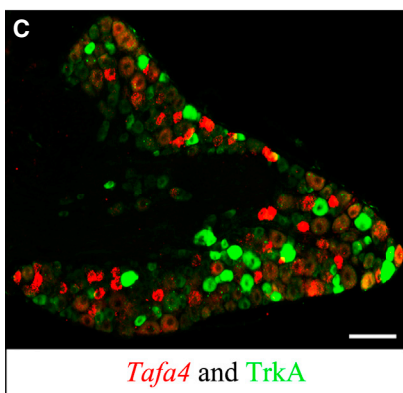
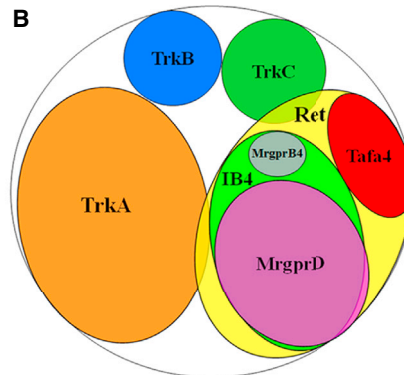
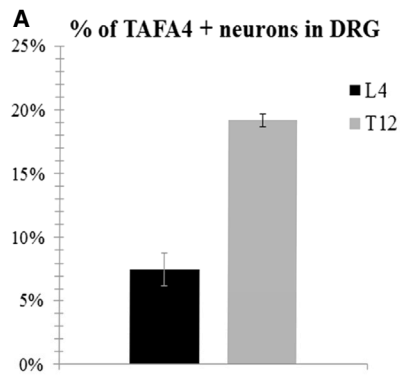


Figure 1. TAF4A Specifically Marks C-LTMRs

(A) Percentage of TAF4A⁺ neurons in L4 (n = 3; 7.5% ± 1.3%) and T12 (n = 3; 19.2% ± 0.5%) DRG of WT adult mice is shown.

(B) Schematic represents DRG *Tafa4* expression data. The sizes of the circles in the diagram are roughly proportional to the sizes of the cell populations depicted by the different molecular markers.

(C–H) In situ hybridizations for *Tafa4* probe in adult mouse lumbar (C–F) and thoracic (G and H) DRG sections followed by immunostaining or in situ hybridizations for *TrkA* (C), *Ret* (D), *MrgprD* (E), *IB4* (fluorescein-conjugated *G. simplicifolia* IB4-lectin) (F), *TH* (G), and EGFP (H) are presented. Scale bar, 100 μm. See also Figure S1.

marker, we found no difference in the total number of neurons between TFAFA4-null and WT DRGs either at thoracic or lumbar levels (Figure S1D). Consistent with these results, quantification of Ret-, TH-, TrkA-, TrkB-, and TrkC-expressing neurons showed no difference between the two genotypes (Figures S1E and S1F), suggesting that these neurons survived, developed, and matured normally in the absence of TFAFA4. Furthermore, homozygous GFP⁺ neurons invaded the innermost layer of laminae II centrally and connected with hair follicles peripherally, revealing that the lack of TFAFA4 had no effect on central or peripheral axonal extension in vivo (Figures S1I–S1J).

To determine whether TFAFA4 modulates neuronal excitability of C-LTMRs, patch-clamp whole-cell recordings were performed on cultured heterozygous and homozygous GFP⁺ neurons. We found no difference in membrane capacitance or cell input resistance (Figure 2C). Loss of TFAFA4 had no effect on the distribution or the density of the different MA currents (Figure 2D), and AP properties of TFAFA4-null neurons were indistinguishable from those of TFAFA4^{GFP/+} (Figures 2E and 2F). Injection of depolarizing current pulses of increasing amplitudes revealed no significant difference in the tonic discharge properties (Figure 2G). Finally, there was no significant difference in the threshold of AP generation, the latency to generate the second AP, and the total number of APs at any given current intensity (Figures 2H and 2I). Together, these results suggest that TFAFA4 is dispensable for the developmental specification and physiological function of the class of neurons expressing this secreted protein.

TFAFA4-Null Mice Develop Severe Injury-Induced Mechanical and Chemical Hypersensitivity

To gain insights into the functional role of TFAFA4 in C-LTMRs, we subjected TFAFA4-null mice to a large battery of somatosensory tests under acute, inflammatory, and neuropathic pain conditions. TFAFA4-null mice appeared normal in terms of body weight, open field (Figure S3A), and rotarod (Figure S3B) profiles, demonstrating that TFAFA4-null mice do not have abnormalities in motor activity or anxiety. We found no difference between WT and TFAFA4-null mice in the hot plate (Figure S3C), thermotaxis gradient assay (Figure S3D), or Hargreaves' test (Figure S3E) as well as in the cold plate, the two temperatures' choice, and the dynamic cold and hot plate tests (data not shown). We then tested TFAFA4-null mice for the ability to sense mechanical stimuli under inflammatory and neuropathic conditions. In both paradigms, acute mechanical sensation was unaffected in TFAFA4-null mice (Figures 3A–3H). In the Carrageenan model, TFAFA4-null mice exhibited drastically prolonged pain hypersensitivity in response to all tested filaments. Indeed, whereas carrageenan-induced mechanical hypersensitivity started returning to baseline levels at day 3 postinflammation in WT mice, mechanical hypersensitivity persisted up to 21 days in TFAFA4-null mice (Figures 3A–3C). Very interestingly, 6 days postinflammation, a time at which we have a highly significant difference between WT and TFAFA4-null mice, IT injection of 2 μ g of recombinant TFAFA4 completely reversed mechanical hypersensitivity of TFAFA4-null mice to WT levels. Importantly, injection of TFAFA5, another member of the TFAFA family, had no effect in TFAFA4-null mice (Figure 3D), highlighting the specificity

of Tafa4. We then sought to test whether TFAFA4 could trigger the same effects observed in TFAFA4-null mice in a WT context. To test this, we used pure C57/Bl6 mice. As shown in Figure 3E, 6 hr postinflammation, IT administration of TFAFA4 but not of TFAFA5 reversed carrageenan-induced mechanical hypersensitivity to baseline levels. At day 1 postinflammation (18 hr after TFAFA4 administration), TFAFA4 effect totally disappeared because mechanical threshold returned back to the level before TFAFA4 IT injection. Interestingly, IT administration of TFAFA4 did not affect the baseline threshold response of naive mice (Figure S3G). Finally, to assess the role of TFAFA4 in neuropathic pain, we used the chronic constriction of the sciatic nerve (CCI) model (Figures 3F–3H). In this paradigm, TFAFA4-null mice also exhibited a prolonged mechanical hypersensitivity phenotype for all tested filaments, and IT administration of recombinant TFAFA4, 30 days after CCI, totally reversed CCI-induced mechanical hypersensitivity in TFAFA4-null mice to WT levels (Figures 3F–3H).

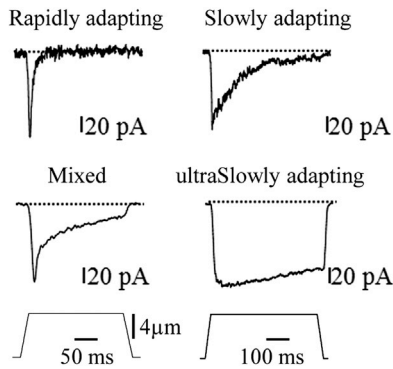
To test whether the enhanced mechanical hypersensitivity in TFAFA4-null mice was modality specific, we carried out the formalin test (Figures 3I and 3J). Intraplantar injection of 10 μ l of 2% formalin triggered a robust first pain response in both genotypes. TFAFA4-null mice exhibited a dramatically elevated response in the second phase, suggestive of an enhanced central sensitization in these mice. Importantly, formalin-induced hypersensitivity in TFAFA4-null mice was reversed to WT levels after IT administration of TFAFA4 15 min before formalin treatment (Figure 3K). Taken together, our results demonstrate that TFAFA4 is required to maintain the normal threshold of injury-induced mechanical and chemical pain hypersensitivity and strongly support a potential role of TFAFA4 as a potent analgesic in the settings of inflammation and neuropathy.

Lamina III Neurons Exhibit Increased Excitability in TFAFA4-Null Mice

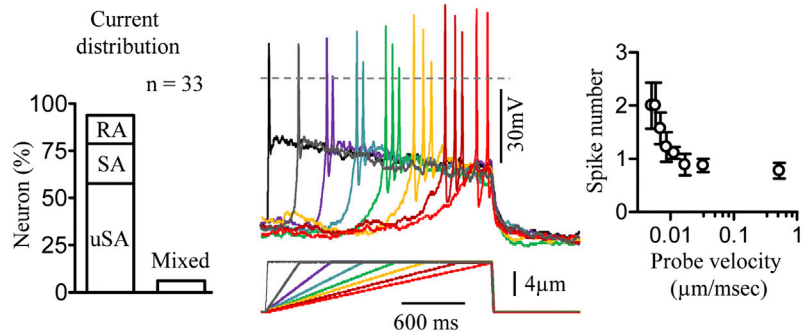
To further explore the central sensitization phenotype induced by the loss of TFAFA4, we performed whole-cell recordings of lamina III neurons in dorsal root-attached spinal cord slices from WT (n = 19) and TFAFA4-null mice (n = 25). We found no difference in average membrane potential, cell input resistance, membrane capacitance, or rheobase (Figures S4A1–S4A4). However, injection of depolarizing current pulses of increasing amplitudes (0–50 pA) elicited more APs in TFAFA4-null neurons than in WT (Figures 4A1 and 4A2; ANCOVA, $p < 0.001$). This effect was even more pronounced at the onset of the depolarizing current pulse because TFAFA4-null neurons showed increased discharge frequency at the beginning of the current pulse, before adapting to discharge rates comparable with those of WT neurons (Figure 4A3). Furthermore, injection of hyperpolarizing current pulses (–50 or –25 pA) elicited higher rebound AP in TFAFA4-null neurons compared to WT (Figures 4A1 and 4A4; $p = 0.049$ and $p = 0.001$, respectively). Together, these data suggest an increased excitability of lamina III neurons in TFAFA4-null mice.

The differences observed in TFAFA4-null mice suggest a differential regulation of slowly inactivating low-threshold currents. To characterize these currents, we measured the outward current elicited at –40 mV in lamina III neurons using a symmetrical

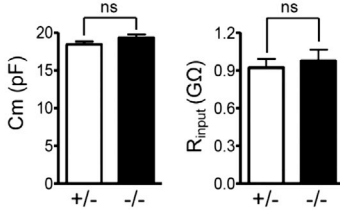
A Mechanically activated cation currents



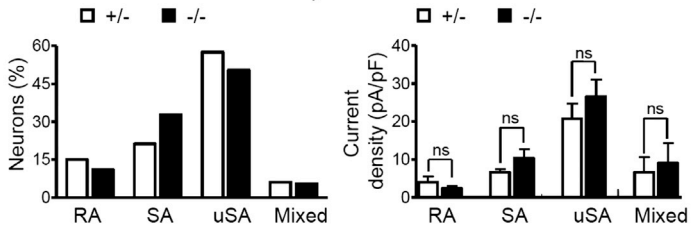
B Mechanically triggered AP



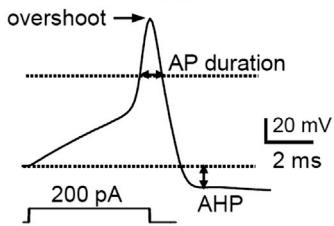
C Passive properties



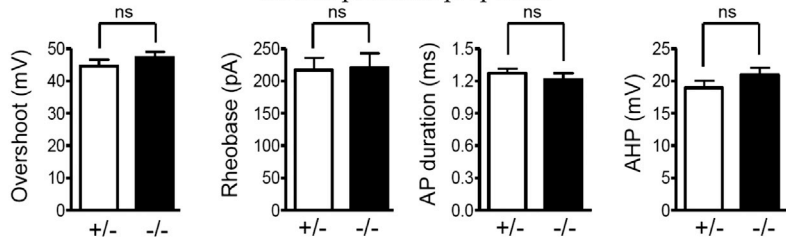
D Mechanically-activated cation currents



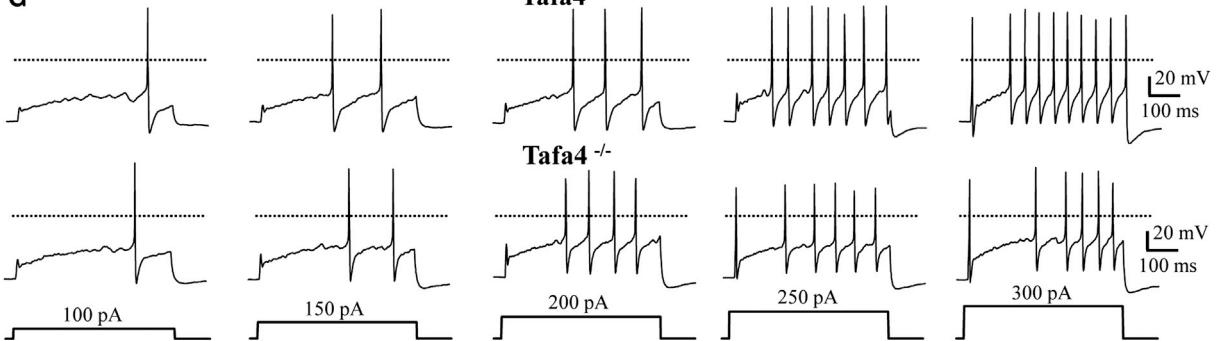
E Tafa4 -/-



F Action potential properties

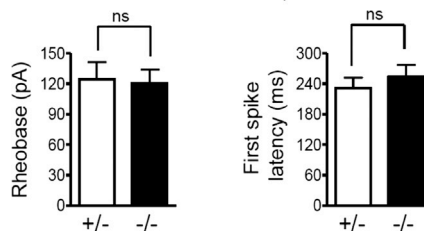


G Tafa4 +/-

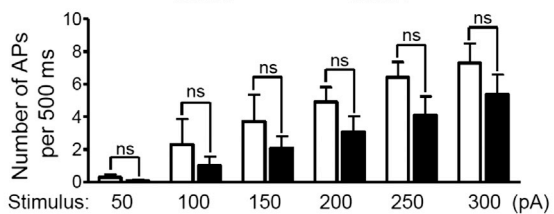


Tafa4 -/-

H 500 ms -steps



I Tafa4 +/- Tafa4 -/-



(legend on next page)

voltage ramp protocol (−40 to −120 mV and back to −40 mV). Whereas in WT neurons, an outward current with slow desensitization could be observed at the end of the rising voltage ramp; this current was almost absent in TFAFA4-null neurons (Figures 4B1 and 4B2; $p = 0.001$). Because IT-administered recombinant TFAFA4 diminishes the exaggerated pain behavior in injured TFAFA4-null mice, we examined the effects of adding recombinant human TFAFA4 on lamina Ili neurons from TFAFA4-null mice. We found that exogenous application of TFAFA4 (20–30 min, 20 nM) induced the expression of an outward current, similar to that observed in neurons from WT animals in control conditions (i.e., without TFAFA4) (Figures 4C1 and 4C2, $n = 19$; $p < 0.001$). This current was not affected by external TEA (2.5 mM, $n = 3$) but was completely blocked by 4AP (1 mM), suggesting A-type current pharmacology. These effects were specific to TFAFA4 because addition of recombinant TFAFA5 ($n = 5$, Figures 4D1 and 4D2) or TFAFA2 ($n = 6$, Figure 4D2) could not elicit this low-threshold outward current from TFAFA4-null neurons.

Following TFAFA4 addition, the distribution of outward current intensities among lamina Ili neurons was best fitted by a mix of two Gaussian curves, revealing the existence of two distinct populations: one-third of the neurons displayed significant outward currents, whereas the remaining neurons were weakly or not affected by TFAFA4 bath application (Figure 4E1). Phenotypic characterization of TFAFA4-responsive neurons showed that TFAFA4 elicited similar outward currents both in GAD^+ and GAD^- neurons (Figure 4E2).

Among low-threshold currents, Ih and T-type calcium currents may also shape the firing of lamina Ili neurons. To characterize Ih-like currents in WT and TFAFA4-null mice, we quantified the hyperpolarization-evoked sag by measuring the difference between peak and steady-state potentials in response to a hyperpolarizing current pulse (Figure S4B1). In both genotypes, we found no difference in the distribution of individual points or the quantification of the sag evoked by −50 and −25 pA current pulses (Figures S4B2 and S4B3). In contrast, isolated T-type currents evoked by square potential pulses (see [Experimental Procedures](#)) were frequently weaker in WT than in TFAFA4-null mice (Figure S4C1). Statistical analysis revealed a significant

increase in T-type current densities in TFAFA4-null lamina Ili neurons compared to WT (Figure S4C2; $p = 0.001$). However, addition of human recombinant TFAFA4 did not alter the T-type current density lamina Ili neurons of TFAFA4-null animals (Figures S4C3 and S4C4), suggesting that the differences in T-type currents observed between WT and TFAFA4-null mice may result from compensatory mechanisms rather than from direct action of TFAFA4 on lamina Ili neurons. Taken together, our results indicate that TFAFA4 directly modulates the intensity of low-threshold outward currents in lamina Ili neurons.

DISCUSSION

In this study, we have used a combination of genetic labeling, electrophysiological recording, and behavioral analyses to unravel the functional role of TFAFA4 in C-LTMRs. We showed that $TFAFA4^+$ neurons display many intrinsic physiological properties of mechano-nociceptors. We also showed that TFAFA4 loss of function led to increased injury-induced mechanical and chemical hypersensitivity and enhanced excitability of laminae Ili neurons. Recombinant TFAFA4 is able to reverse injury-induced mechanical and chemical hypersensitivity in a loss of function as well as in a pure WT background. Therefore, TFAFA4 plays an important role in modulating neuronal excitability and the threshold of somatic sensation.

Although discovered many decades ago (Zotterman, 1939), and despite the intense studies regarding their physiological properties, our knowledge of the molecular content, the anatomical organization, and the functional specialization of C-LTMRs is just emerging. Recent studies have shown that C-LTMRs represent a unique population of nonpeptidergic, small diameter sensory neurons that express VGLUT3 and TH (Li et al., 2011; Seal et al., 2009). These neurons project to the innermost layer of lamina II in the spinal cord (Seal et al., 2009), a layer that has been shown to contribute to persistent pain caused by injury (Malmberg et al., 1997), and display an exquisite peripheral and central organization with physiologically distinct subtypes of $A\beta$ and $A\delta$ LTMRs (Li et al., 2011). Our genetic labeling of $TFAFA4^+$ neurons confirmed both findings showing that $TFAFA4^+$ afferents exclusively

Figure 2. Representative Traces of Mechano-Gated Currents and Comparison of the Electrophysiological Properties of $Tafa4^{GFP/+}$ and $Tafa4$ -Null DRG Neurons

(A) Representative traces of MA currents elicited by a standard mechanical stimulus of 8 μm in four different $TFAFA4^{GFP/+}$ neurons are shown. The velocity of the mechanical probe was 800 $\mu\text{m}/\text{s}$ during the forward motion of the mechanical stimulus. Holding potential, −100 mV. Right panel shows frequency distribution of rapidly adapting (RA), slowly adapting (SA), ultraslowly adapting (uSA), and mixed MA currents. Data collected over 33 $TFAFA4^{GFP/+}$ neurons and stimulated with a standard mechanical stimulus of 8 μm are presented.

(B) Velocity-related firing property of a $TFAFA4^{GFP/+}$ neuron is shown. Note that firing was enhanced as mechanical stimuli were applied with slow rates of onset ($n = 7$).

(C) Histograms compare the membrane capacitance (C_m) and the input resistance (R_{input}) of $TFAFA4^{GFP/+}$ ($n = 46$) and $TFAFA4$ -null ($n = 37$) GFP^+ DRG neurons. Bars represent mean \pm SEM. ns, not significant.

(D) Frequency distribution and density of rapidly adapting, slowly adapting, ultraslowly adapting, and mixed MA currents in $TFAFA4^{GFP/+}$ ($n = 33$) and $TFAFA4$ -null ($n = 36$) GFP^+ neurons are shown.

(E) Representative AP is evoked by a short depolarizing current injection in a $TFAFA4$ -null DRG neuron.

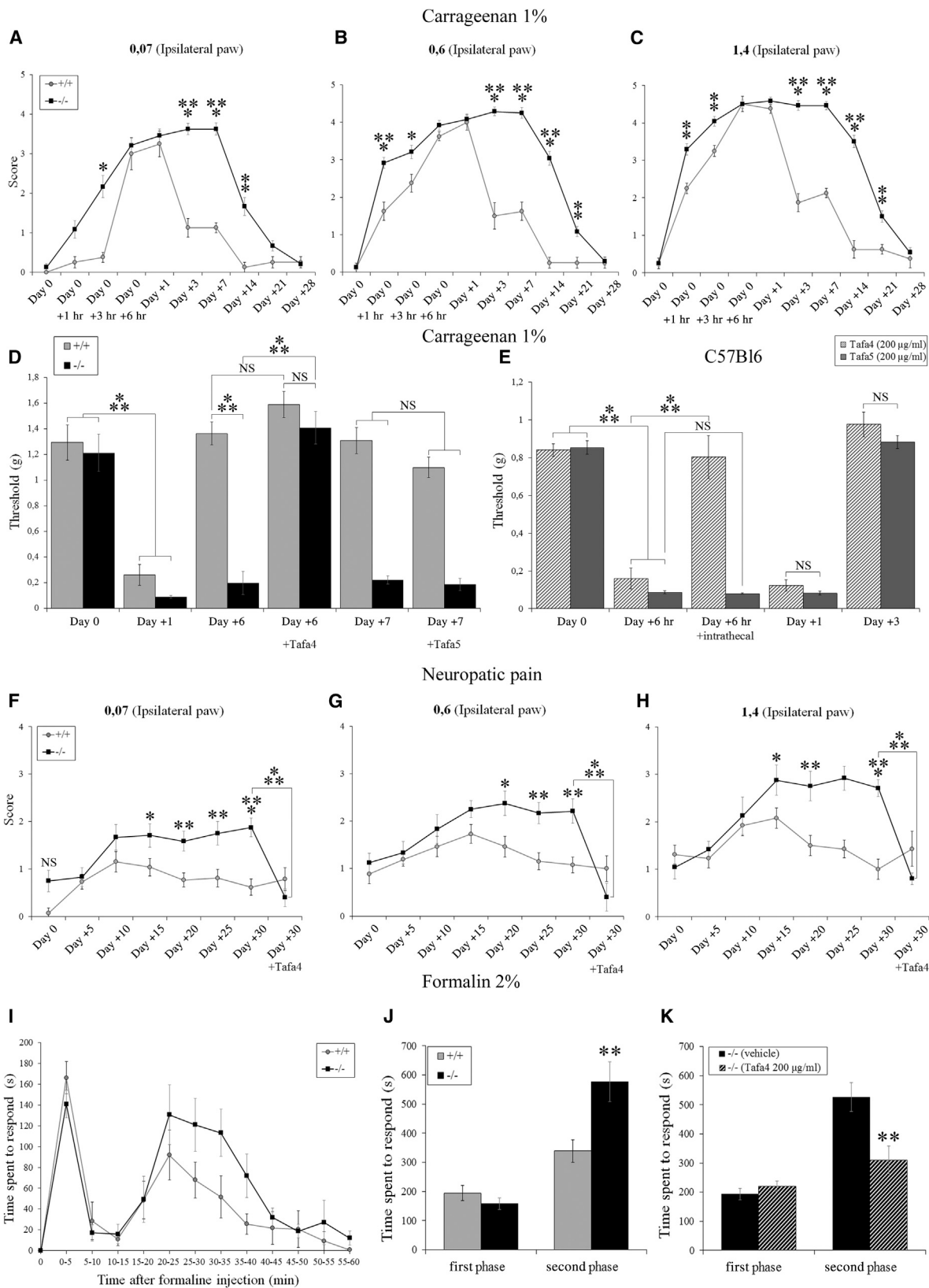
(F) Comparison of AP parameters in $TFAFA4^{GFP/+}$ ($n = 16$) and $TFAFA4$ -null ($n = 15$) neurons as determined in (C) is shown.

(G) Representative recordings of firing discharges evoked in $TFAFA4^{GFP/+}$ and $TFAFA4$ -null GFP^+ neurons by 500 ms depolarizing current injections are presented.

(H) Comparison of the rheobase current (i.e., minimal electric current of 500 ms duration necessary to produce a spike) and first-spike latency in $TFAFA4^{GFP/+}$ ($n = 15$) and $TFAFA4$ -null ($n = 13$) GFP^+ neurons is shown. Data are determined as in (E).

(I) Stimulus-frequency relationships in $TFAFA4^{GFP/+}$ ($n = 7$) and $TFAFA4$ -null ($n = 7$) neurons using 500 ms depolarizing current injections are presented.

See also [Figure S2](#).



(legend on next page)

innervate hair follicles in the periphery and project to the innermost layer of lamina II centrally.

Human psychophysical studies have implicated C-LTMRs in two distinct features of mechanical sensation: sensation of pleasant touch, and sensation of vibration-evoked pain (Löken et al., 2009; Nagi et al., 2011). In the mouse, VGLUT3 loss of function specifically impairs mechanical hypersensitivity following inflammation, nerve injury, and trauma, indicating a critical role of C-LTMRs in the mechanical hypersensitivity caused by injury (Seal et al., 2009). Our behavioral experiments showed that TFAFA4-null mice developed sustained mechanical allodynia and hyperalgesia in the settings of inflammation and nerve injury, suggesting opposite roles of glutamate and TFAFA4 in modulating injury-induced mechanical hypersensitivity. It is tempting to postulate that upon activation, C-LTMRs would release both glutamate and TFAFA4, with glutamate promoting mechanical hypersensitivity, whereas TFAFA4 mainly preventing mechanical hypersensitivity.

The role of VGLUT3 in controlling mechanical hypersensitivity has been recently challenged by a work from Lou et al. (2013) in which RUNX1 has been selectively ablated in C-LTMRs. In these mice, injury-induced mechanical hypersensitivity was similar to control mice even though VGLUT3 expression was drastically impaired, suggesting that VGLUT3 is dispensable for modulating injury-induced mechanical pain. Our study shows that loss of TFAFA4 in C-LTMRs leads to enhanced mechanical hypersensitivity in the settings of inflammation and nerve injury, suggesting that C-LTMR activation plays an important role in controlling the thresholds of somatic sensation. How can one reconcile the discrepancies between these different studies? First, it is well established that RUNX1 is required for the maintenance of the expression of a large cohort of genes in RUNX1-persistent neurons (Chen et al., 2006). Thus, ablation of RUNX1 in C-LTMRs might trigger downregulation of a variety of genes whose expression is required for proper function of C-LTMRs, including TFAFA4. Dual downregulation of VGLUT3 and TFAFA4, which play antagonistic roles, could perfectly explain the phenotype observed in the study by Lou et al. (2013). Second, because of the broad expression of VGLUT3 in the central and peripheral nervous system, conditional inactivation of VGLUT3 specifically in C-LTMRs will allow accurate genetic dissection of the sensory versus central role of VGLUT3 in injury-induced mechanical pain. Regardless, our

study in addition to few other studies (Li et al., 2011; Lou et al., 2013; Seal et al., 2009) provide molecular insights into the development, the exquisite topographic central and peripheral organization, and the functional role of C-LTMRs in mechano-sensation in vivo.

We also found that TFAFA4 modulates the second phase of formalin-evoked pain. However, the neuronal subpopulations and the molecular mechanisms underlying the nocifensive behavior triggered by formalin are still unknown. Recent genetic and chemical neuronal ablation studies suggest that formalin-evoked nocifensive behavior is likely to be triggered by a yet to be identified small subset of DRG neurons (Abrahamsen et al., 2008; Cavanaugh et al., 2009; Shields et al., 2010). Indeed, ablation of a subpopulation of neurons encompassing MRGPRD⁺ and TFAFA4⁺ neuronal subsets significantly reduced the first formalin-evoked pain and completely abolished the second pain response (data not shown). These data, in addition to our observed enhanced formalin-evoked second pain response in TFAFA4-null mice, strongly suggest that C-LTMRs are likely to play a role in modulation of formalin-induced pain.

Genetic marking of Tafa4-expressing neurons allowed detailed in vitro study of the physiological properties of C-LTMRs. Patch-clamp analysis revealed a strikingly homogeneous population of neurons with small capacitance, unique short-duration APs, Nav1.8 currents, and a remarkable coexpression of several low-threshold currents as well as slowly and ultraslowly adapting excitatory mechano-gated currents. Loss of TFAFA4 does not seem to interfere with the excitability of C-LTMRs, potentially indicating the absence of a cell-autonomous role of this secreted protein in this process. However, it remains possible that the lack of significant differences observed in this study might be due to the fact that our experiments compare heterozygous with homozygous GFP⁺ neurons. Indeed, although not significant, Figure 2I shows a tendency of homozygous GFP⁺ neurons to exhibit less APs compared to heterozygous GFP⁺ neurons.

Sensory inputs from the periphery are processed and conveyed to higher brain regions by complex circuits involving excitatory and inhibitory interneurons within the spinal cord (Basbaum et al., 2009; Todd, 2010). The balance between excitation and inhibition is crucial for the maintenance of normal sensory function, and dysfunction of these circuits leads to the development of inflammatory and neuropathic pain. Our

Figure 3. Tissue-Injury-Induced Hypersensitivity Is Increased in TFAFA4-Null Mice

(A–C) Time course shows mechanical sensitivity of TFAFA4-null mice (n = 12) and WT littermates (n = 7) before (Day 0) and following Carrageenan injection using three different filaments of increasing calibers (0.07, 0.6, and 1.4 g).

(D) Time course presents mechanical sensitivity of WT and TFAFA4-null littermates (n = 6) before and after Carrageenan injection using an “up and down method”. At day 6 and day 7, the mechanical threshold was measured before and 15 min after IT injection of 2 μg of human recombinant TFAFA4 or TFAFA5, respectively.

(E) Time course shows mechanical sensitivity of C57Bl6 mice before and following Carrageenan injection. Recombinant TFAFA4 (n = 8) and TFAFA5 (n = 7) were administered at 6 hr postinflammation.

(F–H) Time course presents mechanical sensitivity following CCI of TFAFA4-null mice (n = 12) and WT littermates (n = 13) using three different filaments of increasing calibers (0.07, 0.6, and 1.4 g). Measures were determined before (Day 0) and every 5 days after the CCI. At Day +30, the score is before and 15 min after IT injection of 2 μg of human recombinant TFAFA4 (TFAFA4-null mice [n = 5], WT [n = 7]).

(I and J) Time course and total time (in two phases: first 0–10 min and second 10–60 min) spent in flinching, biting, and licking behavior following 2% formalin injection (WT n = 11 and TFAFA4-null mice n = 12) are shown.

(K) IT injection of 2 μg of human recombinant TFAFA4 restores formalin-evoked hypersensitivity to WT levels in TFAFA4-null mice (vehicle n = 8, TFAFA4 n = 8).

Data are shown as mean ± SEM. *p < 0.05, **p < 0.01, and ***p < 0.001, one-way ANOVA followed by unpaired t test. See also Figure S3.

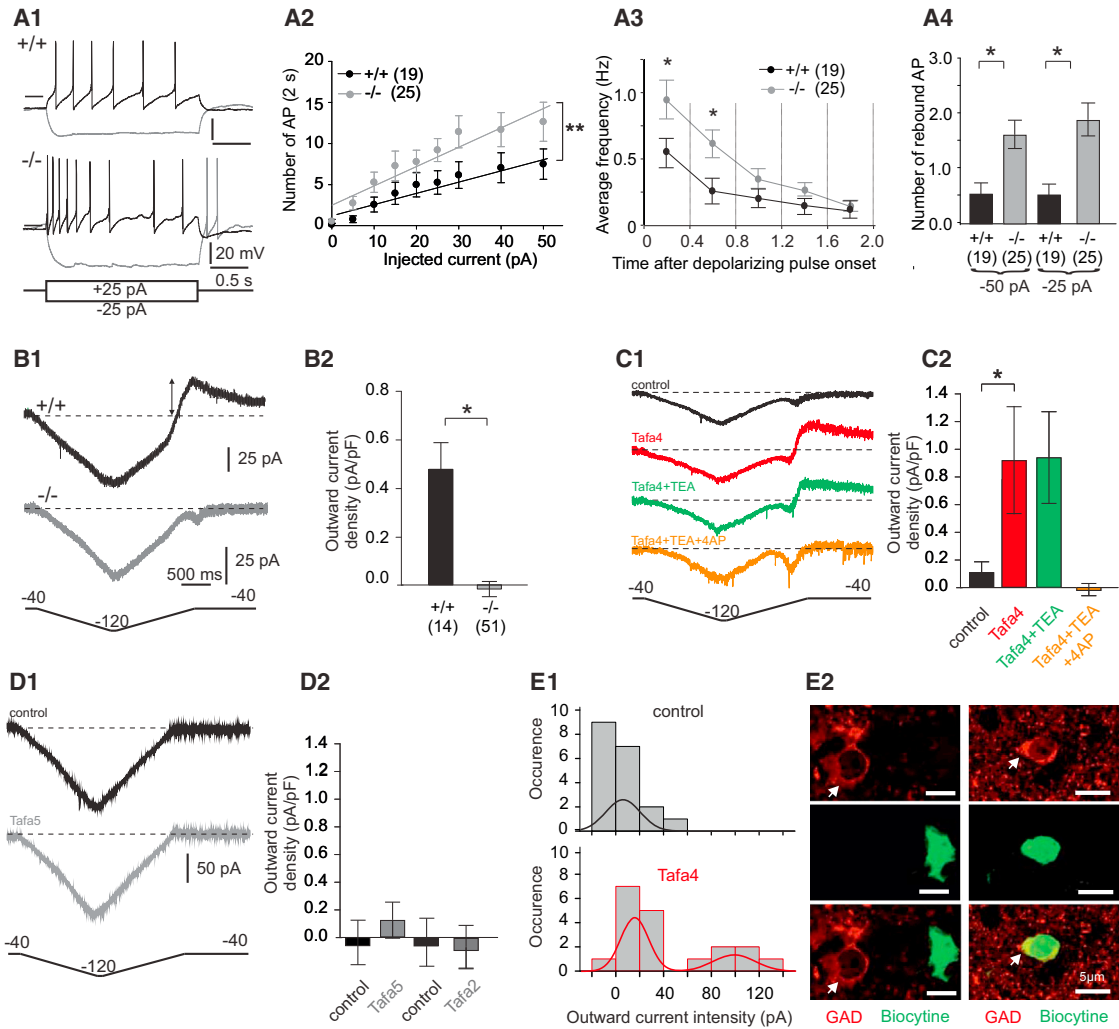


Figure 4. Lamina III Neuron Excitability in TAF4-Null Mice

(A1) Representative recordings show the responses of neurons from WT (top) or TAF4-null (bottom) spinal slices to a 2 s depolarizing (+25) or hyperpolarizing (-25 pA) current pulse.

(A2) Quantification of the average number of APs elicited by current pulses of increasing intensities (5–50 pA). (ANCOVA, $p < 0.01$) is shown.

(A3) Average firing rate at different times of the discharge elicited by a 2 s depolarizing current pulse (+25 pA) in lamina III neurons of WT and TAF4-null mice is presented.

(A4) Average number of rebound APs following a 2 s hyperpolarizing current pulse (-50 and -25 pA) (t test, $p < 0.05$) is shown.

(B1) Representative current responses from WT and TAF4-null neurons to a back-and-forth voltage ramp from -40 to -120 mV are shown. Each trace represents the average of five consecutive responses.

(B2) Quantification of the peak of the outward current measured at the end of the rising voltage ramp in lamina III neurons of WT and TAF4-null animals (t test, $p < 0.05$) is presented.

(C1) Response of a TAF4-null lamina III neuron to a back-and-forth voltage ramp in control conditions and in the presence of 20 nM recombinant TAF4, TEA (2.5 mM), and 4AP (1 mM), is shown.

(C2) Quantification of the outward current measured at the end of the rising edge of the voltage ramp in TAF4-Lamina III neurons is shown. Notice the increase in outward current following TAF4 application ($p < 0.05$), and the blockade of this current by 4AP.

(D1 and D2) Representative traces and quantification of the outward current in lamina III neurons of TAF4-null animals following the bath superfusion of TAF5 and TAF2 (20 nM each) are shown.

(E1) Occurrence of low-threshold outward current in WT and following recombinant TAF4 superfusion is presented.

(E2) Examples of lamina $GAD65^{-}/GAD67^{-}$ (left) and $GAD65^{+}/GAD67^{+}$ (right) neurons are shown. Images are single confocal planes. White arrows indicate the labeling of GAD^{+} soma.

See also Figure S4.

study shows that the loss of TFAFA4 led to enhanced excitability of lamina II neurons. Intriguingly, we found no significant differences in ion channel conductances in the cell soma of cultured TFAFA4-null GFP⁺ neurons compared to TFAFA4^{GFP/+} neurons. Nonetheless, it is conceivable that TFAFA4 could acutely regulate presynaptic channels in primary afferents that in turn increase synaptic transmission. Postsynaptically, the “TFAFA4ergic” C-LTMR afferents face a network of lamina II excitatory glutamatergic and inhibitory GABAergic/glycinergic interneurons that are connected to projection neurons residing in lamina I. Although this wiring is not fully understood, we propose an attractive hypothesis in which, in a WT situation, under pathological conditions, elevated neuronal activity in C-LTMRs would enhance tonic secretion of TFAFA4 that will depress a subset of glutamatergic excitatory and GABAergic inhibitory interneurons, through the activation of a low-threshold outward current. Because excitatory transmission dominates sensory processing in substantia gelatinosa (Santos et al., 2007), the net result of this dual depression of GAD⁺ and GAD⁻ cells would be dominated by a decrease in excitatory transmission, thereby reducing the amount of nociceptive information transmitted to lamina I projection neurons. TFAFA4 effect on excitatory and inhibitory interneurons is not surprising but rather consistent with previous studies showing other mediators, with strong antinociceptive effects, altering inhibitory and excitatory spinal interneurons (Yasaka et al., 2010). Further work aimed at deciphering the molecular machinery that triggers injury-induced release of TFAFA4 in addition to identification of the receptors through which TFAFA4 exerts its modulatory action on spinal cord interneurons will greatly advance our understanding of the role of C-LTMR-derived TFAFA4 in pain processing.

EXPERIMENTAL PROCEDURES

Generation of *tafa4-GFP KI* Mice

To generate *tafa4-GFP KI* mice, we used the bacterial artificial chromosome (BAC)-based homologous recombination in embryonic stem cells. Details are available in [Supplemental Experimental Procedures](#).

In Situ Hybridization and Immunofluorescence

In situ hybridization and immunofluorescence were performed following standard protocols (Moqrich et al., 2004). RNA probes (*Tafa4*, *TH*, *Vglut3*, *TrkB*, *MrgprD*, and *SCG10*) were synthesized using gene-specific PCR primers and cDNA templates from embryonic or adult mouse DRG. Primary antibodies, neuronal counts, and statistical analyses are described in [Supplemental Experimental Procedures](#).

Electrophysiological Recording and Calcium Imaging

Whole-cell patch-clamp recordings of cultures of DRG neurons and from spinal cord slices with attached dorsal root as well as calcium-imaging protocols are described in [Supplemental Experimental Procedures](#).

Behavioral Assays

All behavior analyses (open field, rotarod, hot plate, cold plate, thermal gradient, two-temperature choice, thermal nociceptive threshold [Hargreaves' test], itch test, Von Frey, dynamic Von Frey, and formalin test) were conducted on littermate males 8–12 weeks old. A detailed description of all these tests is provided in [Supplemental Experimental Procedures](#). Complete Freund's adjuvant (CFA) and Carrageenan hindpaw injection, IT injection of recombinant TFAFA4 and TFAFA5, and CCI are also described in [Supplemental](#)

[Experimental Procedures](#). The Student's t test was used for all statistical calculations.

SUPPLEMENTAL INFORMATION

Supplemental Information includes Supplemental Experimental Procedures and four figures and can be found with this article online at <http://dx.doi.org/10.1016/j.celrep.2013.09.013>.

AUTHOR CONTRIBUTIONS

A. Moqrich designed the project. M.-C.D. and A. Mantilleri generated the knockin mouse model. M.-C.D., A. Mantilleri, and S.G. performed functional characterization of TFAFA4 mice. S.A. performed southern blot screening. J.H., P.D., C.B., A.F., E.B., M.L., and Y.L.F. performed calcium imaging and electrophysiological experiments. R.S. provided perfused DRGs from VGLUT3-EGFP mice. A.R. and A. Mantilleri performed Eliza experiments. A.A. and A.E. performed the CCI experiments. P.M. provided logistical help. M.-C.D., A. Mantilleri, and A. Moqrich wrote the paper.

ACKNOWLEDGMENTS

We are grateful to the CIML transgenic core facility for generation of *tafa4-GFP KI* chimeric mice. Thanks to L.F. Reichardt for providing TrkA antibody. We also thank N. Lalevée and the members of the laboratory for scientific discussions, IBDMML imaging, and animal facilities for assistance. A. Mantilleri was a BDE-Region (Région Provence-Alpes-côte d'Azur) fellow cosponsored by Bioseb. This work has been funded by ANR-Nociceptor diversity and ERC-Starting grant paineurons 260435.

Received: June 15, 2013

Revised: July 26, 2013

Accepted: September 9, 2013

Published: October 17, 2013

REFERENCES

- Abrahamsen, B., Zhao, J., Asante, C.O., Cendan, C.M., Marsh, S., Martinez-Barbera, J.P., Nassar, M.A., Dickenson, A.H., and Wood, J.N. (2008). The cell and molecular basis of mechanical, cold, and inflammatory pain. *Science* **321**, 702–705.
- Basbaum, A.I., Bautista, D.M., Scherrer, G., and Julius, D. (2009). Cellular and molecular mechanisms of pain. *Cell* **139**, 267–284.
- Bessou, P., and Perl, E.R. (1969). Response of cutaneous sensory units with unmyelinated fibers to noxious stimuli. *J. Neurophysiol.* **32**, 1025–1043.
- Bessou, P., Burgess, P.R., Perl, E.R., and Taylor, C.B. (1971). Dynamic properties of mechanoreceptors with unmyelinated (C) fibers. *J. Neurophysiol.* **34**, 116–131.
- Cavanaugh, D.J., Lee, H., Lo, L., Shields, S.D., Zylka, M.J., Basbaum, A.I., and Anderson, D.J. (2009). Distinct subsets of unmyelinated primary sensory fibers mediate behavioral responses to noxious thermal and mechanical stimuli. *Proc. Natl. Acad. Sci. USA* **106**, 9075–9080.
- Chen, C.L., Broom, D.C., Liu, Y., de Nooij, J.C., Li, Z., Cen, C., Samad, O.A., Jessell, T.M., Woolf, C.J., and Ma, Q. (2006). Runx1 determines nociceptive sensory neuron phenotype and is required for thermal and neuropathic pain. *Neuron* **49**, 365–377.
- Douglas, W.W., and Ritchie, J.M. (1957). Nonmedullated fibres in the saphenous nerve which signal touch. *J. Physiol.* **139**, 385–399.
- Johansson, R.S., Trulsson, M., Olsson, K.A., and Westberg, K.G. (1988). Mechanoreceptor activity from the human face and oral mucosa. *Exp. Brain Res.* **72**, 204–208.
- Legha, W., Gaillard, S., Gascon, E., Malapert, P., Hocine, M., Alonso, S., and Moqrich, A. (2010). *stac1* and *stac2* genes define discrete and distinct subsets of dorsal root ganglia neurons. *Gene Expr. Patterns* **10**, 368–375.

- Li, L., Rutlin, M., Abraira, V.E., Cassidy, C., Kus, L., Gong, S., Jankowski, M.P., Luo, W., Heintz, N., Koerber, H.R., et al. (2011). The functional organization of cutaneous low-threshold mechanosensory neurons. *Cell* 147, 1615–1627.
- Liljencrantz, J., Björnsdotter, M., Morrison, I., Bergstrand, S., Ceko, M., Seminowicz, D.A., Cole, J., Bushnell, M.C., and Olausson, H. (2013). Altered C-tactile processing in human dynamic tactile allodynia. *Pain* 154, 227–234.
- Löken, L.S., Wessberg, J., Morrison, I., McGlone, F., and Olausson, H. (2009). Coding of pleasant touch by unmyelinated afferents in humans. *Nat. Neurosci.* 12, 547–548.
- Lou, S., Duan, B., Vong, L., Lowell, B.B., and Ma, Q. (2013). Runx1 controls terminal morphology and mechanosensitivity of VGLUT3-expressing C-mechanoreceptors. *J. Neurosci.* 33, 870–882.
- Lumpkin, E.A., Marshall, K.L., and Nelson, A.M. (2010). The cell biology of touch. *J. Cell Biol.* 191, 237–248.
- Malmberg, A.B., Chen, C., Tonegawa, S., and Basbaum, A.I. (1997). Preserved acute pain and reduced neuropathic pain in mice lacking PKC γ . *Science* 278, 279–283.
- Maruhashi, J., Mizuguchi, K., and Tasaki, I. (1952). Action currents in single afferent nerve fibres elicited by stimulation of the skin of the toad and the cat. *J. Physiol.* 117, 129–151.
- Moqrich, A., Earley, T.J., Watson, J., Andahazy, M., Backus, C., Martin-Zanca, D., Wright, D.E., Reichardt, L.F., and Patapoutian, A. (2004). Expressing TrkC from the TrkA locus causes a subset of dorsal root ganglia neurons to switch fate. *Nat. Neurosci.* 7, 812–818.
- Nagi, S.S., Rubin, T.K., Chelvanayagam, D.K., Macefield, V.G., and Mahns, D.A. (2011). Allodynia mediated by C-tactile afferents in human hairy skin. *J. Physiol.* 589, 4065–4075.
- Olausson, H., Lamarre, Y., Backlund, H., Morin, C., Wallin, B.G., Starck, G., Ekholm, S., Strigo, I., Worsley, K., Vallbo, A.B., and Bushnell, M.C. (2002). Unmyelinated tactile afferents signal touch and project to insular cortex. *Nat. Neurosci.* 5, 900–904.
- Santos, S.F., Rebelo, S., Derkach, V.A., and Safronov, B.V. (2007). Excitatory interneurons dominate sensory processing in the spinal substantia gelatinosa of rat. *J. Physiol.* 581, 241–254.
- Seal, R.P., Wang, X., Guan, Y., Raja, S.N., Woodbury, C.J., Basbaum, A.I., and Edwards, R.H. (2009). Injury-induced mechanical hypersensitivity requires C-low threshold mechanoreceptors. *Nature* 462, 651–655.
- Shields, S.D., Cavanaugh, D.J., Lee, H., Anderson, D.J., and Basbaum, A.I. (2010). Pain behavior in the formalin test persists after ablation of the great majority of C-fiber nociceptors. *Pain* 151, 422–429.
- Smith, E.S., and Lewin, G.R. (2009). Nociceptors: a phylogenetic view. *J. Comp. Physiol. A Neuroethol. Sens. Neural Behav. Physiol.* 195, 1089–1106.
- Todd, A.J. (2010). Neuronal circuitry for pain processing in the dorsal horn. *Nat. Rev. Neurosci.* 11, 823–836.
- Tom Tang, Y., Emtage, P., Funk, W.D., Hu, T., Arterburn, M., Park, E.E., and Rupp, F. (2004). TAFAs: a novel secreted family with conserved cysteine residues and restricted expression in the brain. *Genomics* 83, 727–734.
- Vrontou, S., Wong, A.M., Rau, K.K., Koerber, H.R., and Anderson, D.J. (2013). Genetic identification of C fibres that detect massage-like stroking of hairy skin in vivo. *Nature* 493, 669–673.
- Woodbury, C.J., Ritter, A.M., and Koerber, H.R. (2001). Central anatomy of individual rapidly adapting low-threshold mechanoreceptors innervating the “hairy” skin of newborn mice: early maturation of hair follicle afferents. *J. Comp. Neurol.* 436, 304–323.
- Yasaka, T., Tiong, S.Y., Hughes, D.I., Riddell, J.S., and Todd, A.J. (2010). Populations of inhibitory and excitatory interneurons in lamina II of the adult rat spinal dorsal horn revealed by a combined electrophysiological and anatomical approach. *Pain* 151, 475–488.
- Zimmermann, K., Hein, A., Hager, U., Kaczmarek, J.S., Turnquist, B.P., Clapham, D.E., and Reeh, P.W. (2009). Phenotyping sensory nerve endings in vitro in the mouse. *Nat. Protoc.* 4, 174–196.
- Zotterman, Y. (1939). Touch, pain and tickling: an electro-physiological investigation on cutaneous sensory nerves. *J. Physiol.* 95, 1–28.